Nanoindentation of cement stone samples

Elena Polonina[1], *Olaf* Lahayne[2], *Josef* Eberhardsteiner[2], *Sergey* Leonovich[1]
[1]Belarusian National Technical University, 220013, Nezavisimosty Ave., 65, Minsk, Belarus
[2]Vienna University of Technology, A-1040, Karlsplatz 13, Vienna, Austria

Abstract. The preliminary results of the studied cement samples were obtained by the nanoindentation method. It was revealed that the elastic modulus M increases in samples that contain a complex additive containing nanosized particles. The effect is also observed with the introduction of an additive containing only one type of nanoparticles (nanosilica sol SiO_2 or carbon nanomaterial MCNT). The selection of the parameters of the nanoindentation method, which ensured the obtaining of the final consistent results, was performed. These results are presented by histograms of the distribution of nanoindentation points in modulus of elasticity M and hardness H and distributions in M and H in the horizontal XY plane perpendicular to the motion of the nanoindentor. The results obtained indicate that there is a change in the nanostructure of the C – S – H gel, which is compared with an increase in strength, Young's moduli and shear, upon the introduction of SiO_2 nanoparticles and MCNT nanoparticles.
Key words: complex nanodispersed additive, nanoindentation method, cement samples.

1 Introduction

Higher requirements for the mechanical properties of materials began to appear. The development of various technologies has become widespread in the modern world, which has contributed to the creation of new building materials. The nanoindentation method has become an alternative approach to studying the mechanical properties of materials at the nanoscale. In this case, it is not the sample size that decreases, but the size of the deformed region. During nanoindentation, most solid and superhard nonmetallic materials are deformed elastically-plastically, which makes it possible to characterize such mechanical properties as hardness and elastic modulus.

Based on the analysis of literature sources, it was revealed that C-S-H exists in at least three structurally different forms: low, high and ultra-high densities, which have different average values of hardness and hardness and different volumetric concentrations. The average values of the stiffness and hardness of various forms of CSH gel turned out to be properties inherent in the C – S – H structure, which do not change in various materials based on Portland cement [1]. Nanoparticles of different chemical composition with high specific surface area and high surface energy are used to target the CSH gel nanostructure. The results of such an influence are studied by a set of methods: calorimetry, thermogravimetry, IR

*Corresponding author:grushevskay_en@tut.by

spectroscopy, X-ray phase analysis, small-angle neutron scattering, scanning and tunneling electron microscopy, atomic force microscopy, nanocondensation, etc. [1-9,13,14-21].

The nanoindentation method makes it possible to assess the effect of nanoparticles directly on the volume fraction of different forms of CSH gel at an early age of 6, 12, 15, 24 h and at an adult age of 4-6 months [2-7]. The aim of the work was to determine the effect of hydrothermal SiO_2 nanoparticles with a high density of surface silanol groups Si-OH and MCNT nanoparticles with an acid-activated surface on the CSH gel nanostructure, separately and in combination, on the CSH gel nanostructure.

2 Methods

The method of nanoindentation was used, when a solid needle of a known shape is pressed into the surface of a cement stone sample at a constant speed. When the specified load or indentation depth is reached, the movement stops for a certain time, after which the needle is retracted in the opposite direction. During loading, the load values and the corresponding indenter displacement are recorded. The resulting relationship is called the loading / unloading curve. From this experimental curve, the hardness and elastic modulus of the material can be determined (a method proposed by Oliver and Far).

In this work, the studies were carried out by an automated Hysitron TI 950 TriboIndenter nanoindenter (a type of nanoindenter with a Berkovich tip with a cone angle of 143 degrees). For mechanical measurements, a diamond probe tip was used.

When constructing the histograms, the M step was 1.5 GPa (m = 100 intervals within 0-150 GPa), the H step was 0.1 GPa (100 intervals within 0-10 GPa).

The results are presented as histograms of the distribution of nanoindentation points in terms of the reduced modulus of elasticity M and hardness H. Deconvolution in three phases J = 1, 2, 3 values x = M, H was performed according to the Gaussian normal distribution for each J-th phase

$$p_j(x) = \frac{1}{\sqrt{2\pi S_J^2}} \exp\left(-\frac{(x-\mu J)^2}{2S_J^2} \right) \quad (1)$$

where μ_J is the mean value of M, H of the J-th phase, s_J is the standard deviation of the distribution in the J-th phase (StdDev). The theoretical probability density function P (x) of the distribution of M, H values was determined taking into account the volume fraction f_J of each phase:

$$P(x) = \sum_{J=1}^{n} f_J p_J(x) \quad (2)$$

where J = 1, 2, 3.

The unknown values of μ_J, s_J, f_J were found from the condition of the minimum of the root-mean-square deviation between the experimental discrete values of the nanoindentation of the probability density Pi and the theoretical values of P (x_j) in each i-th interval under the additional condition that the sum of the volume fractions of the phases f_J is equal to one (m = 100 is the number intervals along the M, H axis) [6]:

$$\min \sum_{i=1}^{m} \frac{\left(P_i - P(x_i)\right)^2}{m} \quad (3)$$

$$\sum_{J=1}^{n} f_J = 1 \quad (4)$$

where J = 1, 2, 3.

To find the minimum of function (3) under additional condition (4) and unknown values μ_J, s_J, f_J, we used the algorithm of the MathLab program.

During the research, the following materials were used as the main components: binder - Portland cement PC 500 D0 with the following mineral composition, wt%: C_3S – 58.31, C_2S - 18.38, C_3A – 8.01, C_4AF - 10.64. Modifying substances: sol of nanosilica (NC) with the following characteristics: SiO_2 content in ash -120 g / dm^3, density ρ = 1075 g / dm^3, total salt content - 1720 mg / dm^3, pH = 9.2, specific surface area 500 m^2 / g and average diameter of primary SiO_2 nanoparticles 5.5 nm; carbon nanomaterial (CNM): average diameter of tubes and fibers 10-300 nm, average length of tubes and fibers 0.01-20 microns, bulk density 0.15-0.22 g / cm^3, ash content no more than 5%, specific adsorption surface from 60 m^2 / g. Superplasticizer (SP) in the form of an aqueous solution is a polycarboxylate copolymer with a density of 1.1-1.14 g / ml, pH = 6-8, a viscosity of 230-330 cps, a content of non-volatile substances of 39-41%, a water-reducing capacity of over 40%. Water for mixing and subsequent hardening.

Tests by the nanoindentation method and ultrasonic measurements were carried out on cement specimens with dimensions of 10x10x20 mm.

The tests were carried out on 4 compositions: Sample № 1 - contains an additive of superplasticizer, Sample № 2 - containing an additive SP + sol of nanosilica SiO_2, Sample № 3 - containing an additive of superplasticizer SP + carbon nanomaterials, Sample № 4 - containing an additive of superplasticizer SP + SiO_2 + CNM

The additive for samples № 1-4 was introduced in the amount of 0.8% by weight of cement. The amount of mixing water for all samples was selected in such a way as to obtain a dough of normal density in all cases. Samples were made from cement paste of normal density. The water-cement ratio of samples 1-4 was W / C = 0.21, the age at nanoindentation and plotting of histograms was 3 months.

The results of our own studies of samples of heavy concrete [8], a complex nanodispersed system (containing an additive of the superplasticizer SP + SiO_2 + CNM), the compressive strength at the age of 28 days reached 78.7 MPa, which exceeds the strength of the control sample by more than 50% and the sample containing only 37% superplasticizer. The difference in compressive strength (fc) between the control sample №1 and modified samples № 2,3 was also established 4. The difference reached at an early age of 1, 3 days - 13 and 12.7%, at the age of 37 days - 11.9%, and was maximum in in the case of using a combination of nanoparticles (SiO_2 + CNM). The difference in bending strength Rben relative to the control was maximum for the sample with a complex addition of NPs (SiO_2 + CNM) and reached at the age of 1, 3 days -39.6 and 21.6%, at the age of 37 days -23.4%.

Based on the results of ultrasonic measurements, reliable increases in Young's modulus E and shear modulus G were obtained at the age of 1 and 5 months in the samples modified with nanoparticles. The maximum increment of 10% was achieved in the variant of modification with a complex nanoadditive (sample № 4).

Nanoindentation first of all shows differences in structure, and such significant differences between samples with nanoparticles № 2, 3, 4 and sample № 1 without nanoparticles have already been identified, and these differences must be attributed to the action of nanoparticles [9-12].

3 Results and discussion

Time schedule of load: 1. immersion up to 300 nm and maximum force for 10 s; 2. constant load mode for 5 s; 3. raising the nanoindenter to the surface, removing the load to 0 within 10 s.

Immersion speed of the nanoindenter: if the maximum immersion depth of the nanoindenter is 300 nm, the immersion time is 10 s, then the immersion speed is 300 nm / 10 s = 30 nm / s.

For each cycle "loading - unloading", a P - h diagram of the dependence of the load on the penetration depth of the indenter was constructed and stored.

The slope of the hysteresis curves in the upper right corner was used to calculate the values of M at the point of indentation; from the maximum load and the area of the contact zone, H was calculated. The calculated values of M and H were used to construct distributions depending on the contact depth of immersion, from the distributions we went to histograms M and H by intervals (Fig. 1), on the basis of equations 3 and 4, the Gaussian functions were found and deconvolution was carried out in three phases (Fig. 1a, b, c, d).

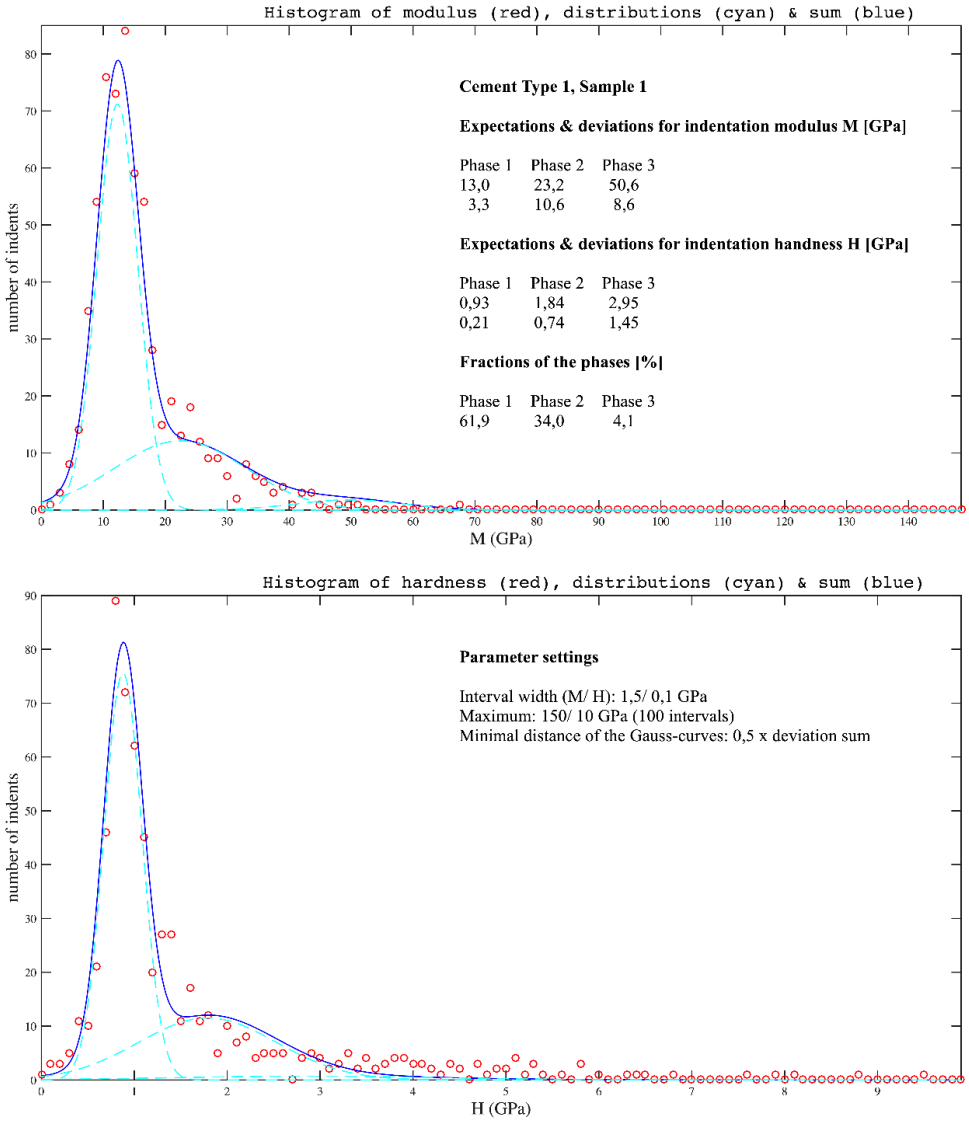

Fig.1a.Histogram of the distribution of nanoindentation points in modulus of elasticity E and hardness H for sample № 1

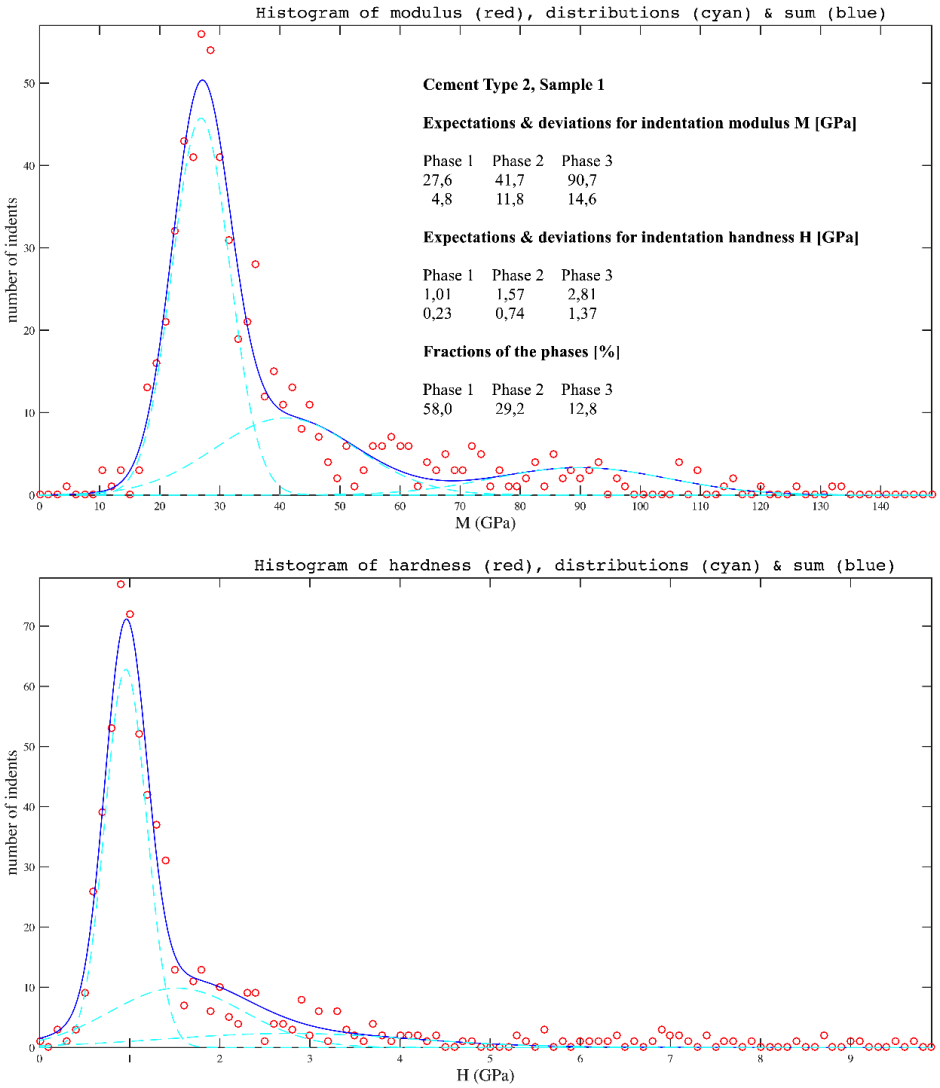

Fig.1b.Histogram of the distribution of nanoindentation points by modulus of elasticity E and hardness H for sample №2

The histograms show phases with their average values of E and H (and moderate statistical scatter within each phase). Then the percentage of each phase was estimated.

The procedure for approximating by Gaussian functions: the starting parameters and the number of phases n are set, and the Matlab program selects the average M and H, the average deviations for each phase, the volume fractions of the phases from the condition of the minimum sum of squares of deviations between the experimental and theoretical points.

The results obtained give a qualitatively correct picture. It is very important that the distribution in the modulus of elasticity M shifted to the right in samples 2, 3, 4 as compared to sample 1. There is also a slight offset to the right in hardness H.

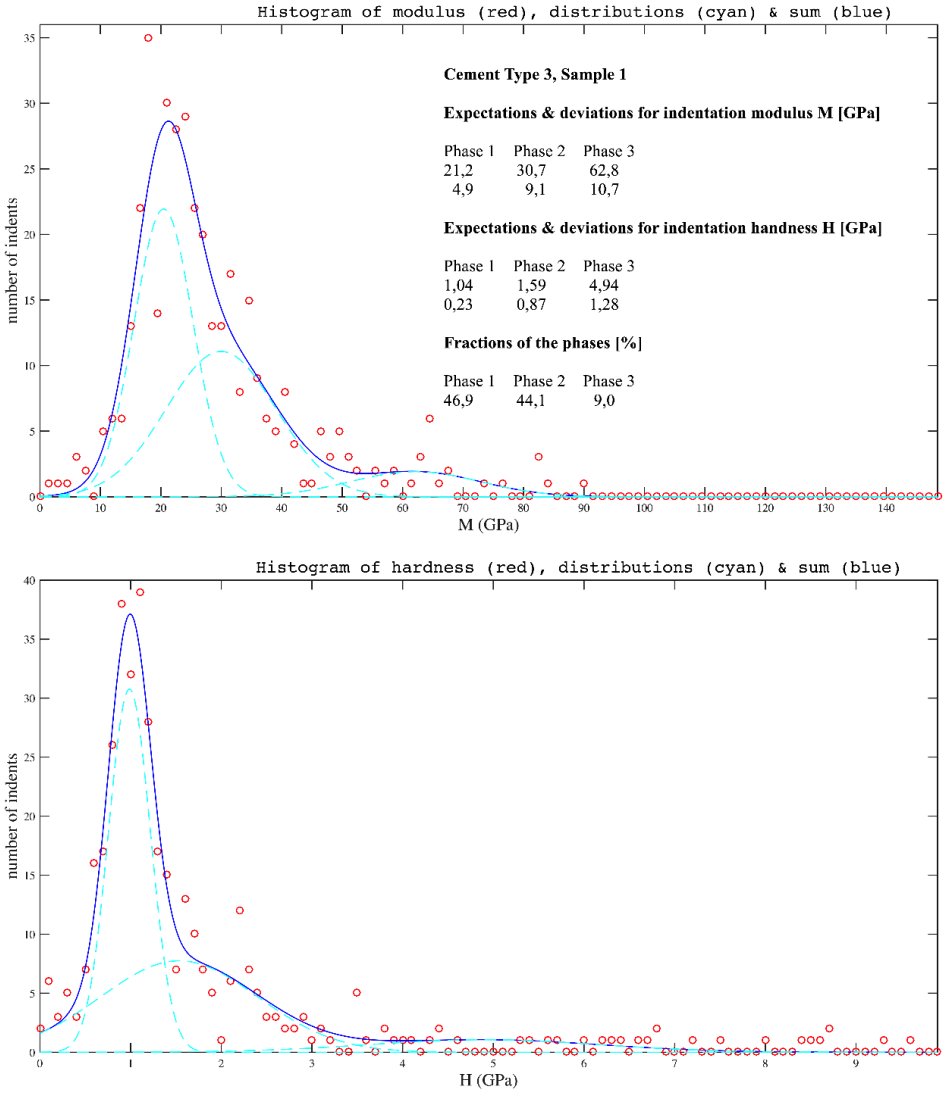

Fig.1c. Histogram of the distribution of nanoindentation points in modulus of elasticity E and hardness H for sample №3

The transition from the distributions M and H to histograms (Fig. 1) showed that the first main maximum for M shifted from the value of 13 GPa for sample № 1 without the introduction of nanoparticles to values in the region of 27.6; 21.2; 22.6 GPa for samples 2, 3 and 4 modified with nanoparticles. The maximum of the second phase in the region of 21.2 GPa for sample № 1 shifted to values of 42.7; 30.7; 36.8 GPa for samples 2, 3, 4. A shift towards higher average values indicates an increase in the volume fraction of the CSH gel phases with a higher packing density of particles and, accordingly, higher mechanical characteristics.

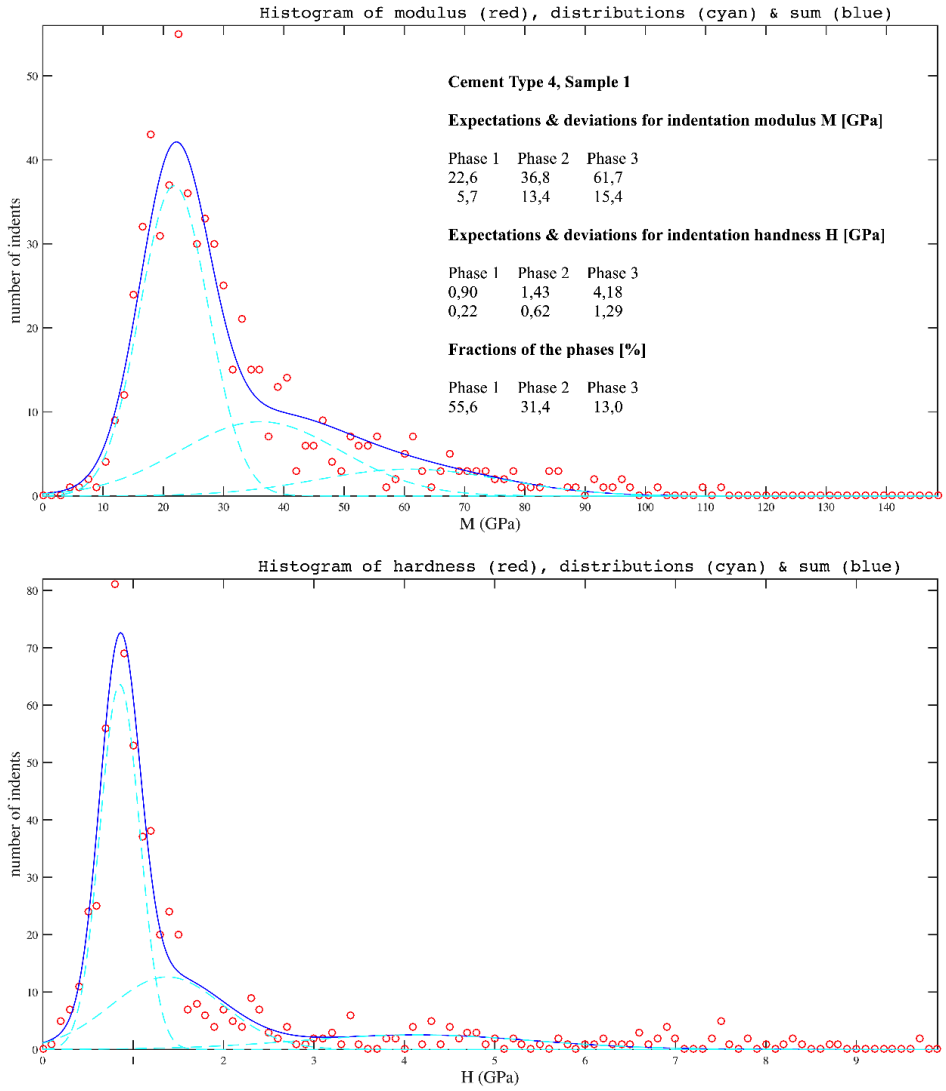

Fig.1d. Histogram of the distribution of nanoindentation points in modulus of elasticity E and hardness H for sample №4

4 Conclusions

1. Obtained hysteresis curves for indentation grid points. For all grid points, the curves were smooth and continuous with a similar shape, which made it possible to calculate the array of M and H values and pass to the distributions of M and H depending on the contact depth of immersion. At the same time, the average immersion depth of about 344 nm provided the following conditions: multiple excess of the minimum size of CSH gel inhomogeneities [6], while having values 10 times smaller than the scale size of the microstructure of the hardening Portland cement sample [6] and 5-fold excess of the size of inhomogeneities of the sample surface (30 nm). The linear dimensions of the indentation area (M) significantly exceeded the scale size of the microstructure of the hardening cement-water sample (1-3 μm). The

number of intervals in the histograms M, H (100) was less than the number of indentation points (595). As a result, these conditions provided a statistically significant set of M, H values, reflecting the inhomogeneous multi-phase structure of the CSH gel - the presence of a number of maxima in the histograms in Fig. 1a-1d with high volume fractions of phases.
2. The shift to the region of higher average values indicates an increase in the volume fraction of CSH gel phases with a higher packing density of particles and, accordingly, higher mechanical characteristics. An increase in the volume of the fraction of the phases of the CSH gel with higher values of M and H corresponds to the results of strength, Young's and shear moduli, and the density of samples of modified SiO_2 nanoparticles and CNM.

References

1. F.Sanchez, K. Sobolev, Vestnik TGASU **3 (40),** pp.262-289 (2013)
2. C. Plassard, E. Lesniewska, I. Pochard, A., Elsevier **100**, pp.331-338 (2004)
3. F.-J. UlmArabian, Journal for Science and Engineering **37(2)**, pp.481–488 (2012)
4. P. Hou, S. Kawashima, ,D. Kong, D. J.Corr, J. Qian, S. P.Shah, Composites Part B: Engineering **45(1)**,pp. 440-448 (2013)
5. J. Eberhardsteiner, S. Zhdanok, B. Khrustalev, E. Batyanovsky, S. Leonovich, P. Samtsov, Science and technology **1**, pp. 52-55 (2012)
6. G. Constantinides, F.J. Ulm, Journal of the Mechanics and Physics of Solids **55(1)**, pp. 64-90 (2007)
7. L.P. Singh, W. Zhu, T. Howind, U. Sharma, Cement & Concrete Composites **(79),** pp. 106-116 (2017)
8. S. Zhdanok, V. Potapov, E. Polonina, S. Leonovich, Engineering Physics Journal **93(3),** pp. 669-673 (2020)
9. V. Potapov, Y. Efmenko, D. Gorev, Nanotechnologies in Construction **11(4)**, pp.308-325 (2019)
10. 10.V. Potapov, E. Grushevskaya, S. Leonovich, Construction Materials, pp.4-9 (2017)
11. S. Zhdanok, E. Polonina, S. Leonovich, B. Khrustalev, E. Koleda, Engineering Physics Journal **92(1)**, pp.14-20 (2019)
12. S. Zhdanok, E. Polonina, S. Leonovich, B. Khrustalev, E. Koleda, Engineering Physics Journal **92(2),** pp.391-396 (2019)
13. L. Krenev, S. Volkov, E. Sadyrin, T. Zubar, S. Chizhik, Engineering Physics Journal **91(3)**, pp.637-644 (2018)
14. U. Sharma, L. Singh., Z. Baojian, C. Poon, Cement and Concrete Composites, pp.312-321 (2019)
15. U. Sharma, L. Singh, D. Ali, C. Poon, Advances in Civil Engineering Materials **8(3)**, pp.346-360 (2019)
16. U. Sharma, D. Ali, L. Singh, European Journal of Environmental and Civil Engineering, pp 1-13 (2019)
17. L. Singh, W. Zhu, T. Howind, U. Sharma, Cement and Concrete Composites **79**, pp.106-116 (2017)
18. I. Flores-Vivian, R. Pradoto, M. Moini, Front. Struct. Civ. Eng. **11**, pp. 436–445 (2017)
19. J. Björnström, A. Martinelli, A. Matic, L. Börjesson, I. Panas, Chemical Physics Letters **392(1–3)**, pp. 242-248 (2004)
20. T. Shi, Y. Gao, P. Surendra, Advances in Cement Research, pp.353-361 (2019)
21. I. Chulkova, I. Selivanov, V. Galdina, Proceedings of universities. Building **10**, pp. 15-27 (2019)